Pressure-induced superconductivity and phonon frequency in paperlike thin films of boron-doped carbon nanotubes

M. Matsudaira,[1] J. Haruyama,[1,2,*] H. Sugiura,[3] M. Tachibana,[3] J. Reppert,[4] A. Rao,[4] T. Nishio,[2] Y. Hasegawa,[2] H. Sano,[2] and Y. Iye[2]

[1]*School of Science and Engineering, Material Science Course, Aoyama Gakuin University, 5-10-1 Fuchinobe, Sagamihara, Kanagawa 229-8558, Japan*

[2]*Institute for Solid State Physics, University of Tokyo, Kashiwanoha 5-1-5, Kashiwa, Chiba 277-8581, Japan*

[3]*International Graduate School of Arts and Science, Yokohama City University, 22-2 Seto, Kanazawa-ku, Yokohama, Kanagawa 236-0027, Japan*

[4]*Department of Physics and Astronomy, Center for Optical Materials Science and Engineering Technologies, Clemson University, Clemson, South Carolina 29634, USA*

(Received 18 March 2010; revised manuscript received 1 June 2010; published 2 July 2010)

We show formation of paperlike thin films (Buckypaper) consisting of pseudo-two-dimensional network of individual boron-doped single-walled carbon nanotubes (B-SWNTs), by sufficiently dissolving as-grown ropes of SWNTs and densely assembling them on silicon substrate. We find superconducting transition at temperature (T_c) of 8 K under absent pressure and that it can be induced as large as 2.4 times up to 19 K by applying a small pressure of 20 MPa. A significant frequency increase in the radial breathing phonon mode (RBM) is also found with applying pressure in Raman spectrum measurements. Moreover, B-SWNTs with a diameter of 0.6 nm are confirmed in the Buckypaper. These imply the strong correlation of the pressure-induced T_c with electron-phonon (RBM) coupling of 0.6-nm-diameter B-SWNTs.

DOI: 10.1103/PhysRevB.82.045402 PACS number(s): 74.70.Wz

I. INTRODUCTION

Recently, thin films consisting of assembled single-walled carbon nanotubes (SWNTs) are attracting considerable attention for application to electrically conductive transparent films, flexible display, and high-mobility flexible electronics using carbon nanotubes (CNTs) field-effect transistors.[1] It is opening up a door for new possibility of CNTs as well as graphene because it requires no exact positioning of individual CNTs on substrates for fabricating electronic circuits and is also easily fabricated even on a plastic substrate. If the thin films are highly conductive, they are much more valuable.

It is well known that ultimately conductive material is superconductor. Indeed, we reported that uniform thin films of boron-doped SWNTs (B-SWNTs) could exhibit Meissner effect at a transition temperature (T_c) of 12 K.[2,3] However, the obtained T_c was still low, in spite that one expects higher T_c for the carbon-based Bardeen-Cooper-Schrieffer-type superconductors due to the high phonon frequency and Debye temperature originating from small mass of carbon atoms. Even in recently developed carbon-based superconductors (e.g., calcium-intercalated graphite and highly B-doped diamond[4–6]), the highest T_c obtained is still now in order of $\sim$10 K (except for pressure-induced T_c of Cs_3C_{60}).

On the other hand, in CNTs, one can expect much higher T_c because (1) the large curvature resulting from a small tube diameter (e.g., $\sim$0.5 nm) can yield sp^3 hybrid orbitals and the σ-π mixture band, resulting in a strong coupling between the σ-π electrons and radial breathing mode (RBM) in phonon[7,8] and (2) the alignment of the Fermi level (E_F) to a Van Hove singularity (VHS) in the one-dimensional electronic density of states (EDOS) can lead to an extremely high EDOS.[8,9] The highest T_c observed in the CNTs,[2,10–12] however, is still 12 K as mentioned above.

In Ref. 2, we reported on synthesis of B-SWNTs by mixing elemental B powder into catalyst in order to intentionally generate charge carriers for superconductivity (SC) and assembling them to thin films. We revealed that (1) B concentration (N_B) as low as 1.5 atomic % (at. %) and (2) assembling into highly uniform films led to Meissner effect with the onset T_c of 12 K. We argued that (1) the better alignment of E_F to a VHS (Refs. 2 and 9) and (2) providing of a loop current path for Meissner diamagnetism across multiple B-SWNTs realized this Meissner effect by the above-mentioned two factors, respectively.[2,11]

Here, in Ref. 2, we had also proposed the following methods for increasing T_c: (1) employing lower N_B values ($N_B \ll 1$ at. %); (2) using thinner B-SWNTs (e.g., diameter $\ll 1$ nm); (3) forming a dense assembly of thin films; and (4) applying pressure to the films. Based on these, in the present study, we report that the onset T_c can be enhanced up to 19 K by applying a small pressure to the Buckypapers consisting of sufficiently dissolved and densely assembled B-SWNTs including 0.6 nm diameter.

II. EXPERIMENTAL

A. Sample preparation

B-SWNTs were synthesized by the pulsed laser vaporization technique[2] in which N_B was controlled by the amount of elemental B mixed with the Co/Ni-catalyst-impregnated targets. Substitutional B doping was confirmed by NMR (JNM-ECX400) and Raman spectra measurements.

Conventional thin-film samples of B-SWNTs (Ref. 2) and the present B-Buckypaper were prepared by solubilizing the B-SWNTs in dichloroethane solution with densities of 0.5–1 mg/mL and 3–5 mg/mL by centrifugation at 5000 rpm for 1 day and 10 000 rpm for 2 days (Tomy; low-speed centri-

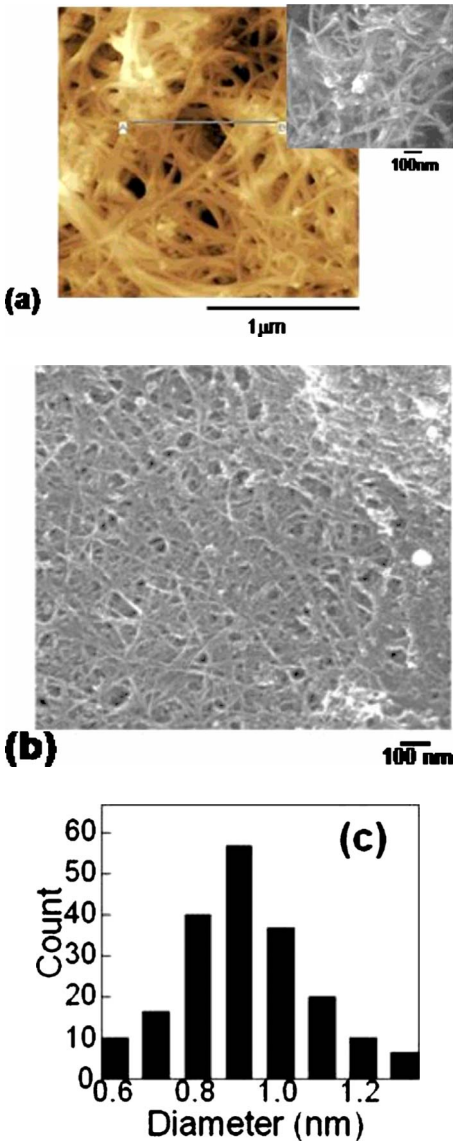

FIG. 1. (Color online) (a) AFM top-view image of conventional thin film of B-SWNTs, which was fabricated by the conditions following our previous method (Ref. 2). Inset: its FESEM image. They include many ropes of as-grown B-SWNTs. (b) FESEM top-view images of the present novel thin film (i.e., Buckypaper) consisting of B-SWNTs without ropes. Buckypaper were formed by assembling densely after sufficient dissolving of as-grown ropes by very strong centrifuges and ultrasonication of the SWNT solution (Ref. 1). (c) Distribution of diameters confirmed by high-resolution transmission electron microscope (HRTEM) observation of individual B-SWNTs used for Buckypaper.

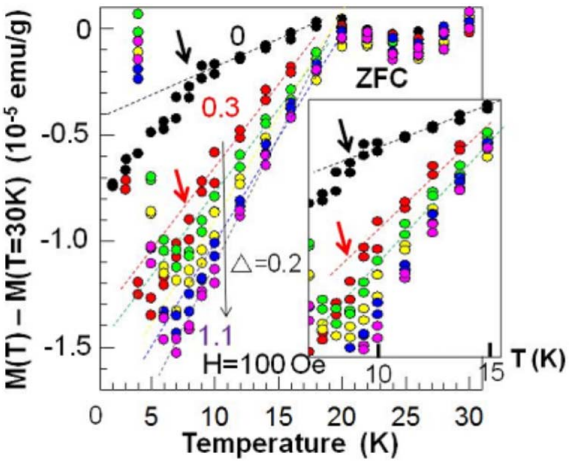

FIG. 2. (Color online) Pressure dependence of normalized magnetization vs temperature relationships for conventional B-SWNT film measured using a superconducting quantum interference device (Quantum Design, MPMS) by embedding the samples in an oil-filled cell for applying pressure. Applied pressure is 0 (black), 0.3 (red), 0.5 (green), 0.7 (yellow), 0.9 (blue), and 1.1 (pink) GPa. Measurements were carried out in two times at individual temperatures. Boron concentration in the catalyst is 1.5 at. %. T_c of this sample is 8 K at zero pressure (shown by arrow). Dotted lines are the results calculated by the method of least squares. Inset: expansion of 5–15 K region of the main panel.

fuge) and ultrasonification (As One, U.S. cleaner) for 2 days and 5 days, respectively. Then, the solutions were spin coated at 500 rpm on a Si substrate.

Figure 1(a) shows the atomic force microscope (AFM) and field-emission scanning electron microscope (FESEM) top-view images of the B-SWNTs thin films prepared by our previous method.[2] They reveal that the film still consists of as-grown thin ropes of B-SWNTs with ~10 nm diameter, which are bundles of SWNTs within strongly intertube van der Waals (IVDW)-coupled triangular lattice in an orderly manner like a graphite.

On the other hand, Fig. 1(b) shows the FESEM image of the present thin film consisting of B-SWNTs, which was fabricated by using much stronger ultrasonication as mentioned above.

This figure is clearly different from Fig. 1(a). It implies the absence of as-grown B-SWNT ropes and indicates that the dissolved SWNTs are assembled into continuous and spread thin film of individual B-SWNTs. The film can be a pseudo-two-dimensional network of IVDW-coupled SWNTs deposited in the form of paper fibers, the so-called Buckypaper.[1]

It is known that the strength of the IVDW coupling in the Buckypaper is weaker than those in as-grown ropes of SWNTs because the Buckypaper was formed by assembling SWNTs in disordered manner once after sufficient dissolving of the as-grown SWNT ropes. SWNTs are not closely packed together into a triangle lattice and some parts of carbon atoms are even within incommensurate state in the Buckypaper.

B. Magnetization measurements

We carried out magnetization measurements on the samples shown in Fig. 1. Figure 2 shows the normalized magnetization $[M_N = M(T) - M(T = 30\ \mathrm{K})]$ of the conventional thin film shown in Fig. 1(a) as functions of temperature (T) and pressure (P) at a magnetic field (H) of 100 Oe in the zero-field-cooled (ZFC) regime. At $P = 0$, an abrupt magnetization drop at T_c of ~8 K (shown by an arrow), which is

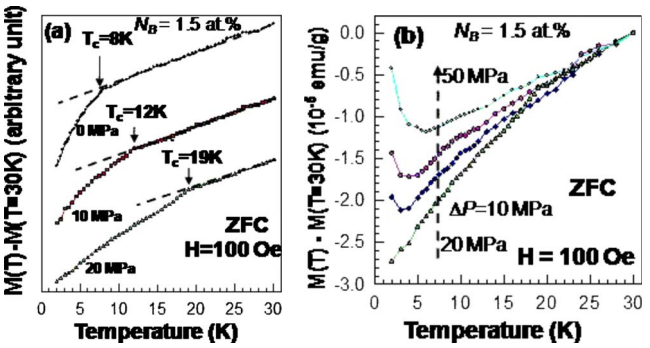

FIG. 3. (Color online) Pressure dependence of normalized magnetization vs temperature relationships of sample shown in Fig. 1(b) (i.e., B-Buckypaper) at (a) $P \leq 20$ MPa and (b) $P \geq 20$ MPa in zero-field-cooled regime. Dotted lines are the results calculated by the method of least squares.

a deviation from dotted line, is evidently observed.

We have confirmed that these magnetization drop observed at $T < T_c$ are attributed to Meissner diamagnetism for type-II SC on the basis of the magnetic field dependence of M_N (i.e., M_N-H relationship) at each temperature as follows[2] while the magnetization drop at $T > T_c$ that appears gradually from high temperatures is due to the graphitic structure of the B-SWNT ropes.

In the Meissner diamagnetism, magnitude of diamagnetism at each temperature increases with an increase in H while it decrease above a critical H value (lower H_c; $H_{c1} = \sim 1500$ Oe in the present sample) and becomes zero at a H value of ~4600 Oe (upper H_c; H_{c2}). This tendency is shown for the Buckypaper in Figs. 3(c) and 3(d).

We have also confirmed mostly linear relationship in the H_{c2} vs T and estimated superconducting coherence length of ~28 nm from the slope value. This is within a reasonable value compared with Ref. 2.

In contrast, in the graphite-originate diamagnetism, magnitude of the diamagnetism monotonically increases with an increase in H. It does not decrease even at very high H values, e.g., as large as ~10 000 Oe. Moreover, this diamagnetism appeared from high temperatures (even from $T = \sim 50$ K), very gradually. They have very different from those in Meissner effect.

Such identifications are shown in Fig. 3 as below and have been used in any present samples for selection of samples with Meissner effect.

Figure 2 indicates that the T_c value of 8 K does not change even at P as large as 0.3 GPa. As P increases further, the graphitic diamagnetism becomes pronounced. Then, T_c corresponding to Meissner diamagnetism becomes no longer apparent. This tendency is also consistent with Fig. 1(a) showing presence of many ropes of B-SWNTs that produce a large graphitic diamagnetism by the strong IVDW coupling because applied pressure drastically induces this graphitic coupling.

On the other hand, Fig. 3 shows the M_N-T relationships for the B-Buckypaper shown in Fig. 1(b) at $P \leq 20$ MPa [Fig. 3(a)] and $P \geq 20$ MPa [Fig. 3(b)] in the ZFC regime. In Fig. 3(a), at $P = 0$, diamagnetism very gradually appears from high temperatures with decreasing temperature while it drastically drops at $T < T_c = 8$ K. In Fig. 4(a), M_N-H relationships for different temperatures at $P = 0$ are shown. Magnitude of diamagnetism at each temperature increases with an increase in H while it decrease above $H_{c1} = \sim 1000$ Oe and becomes zero at H_{c2} value of 4000–5000 Oe.

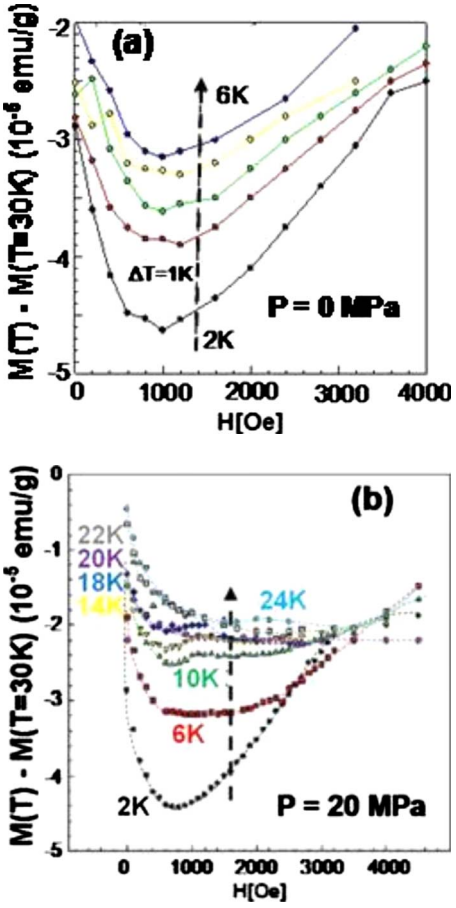

FIG. 4. (Color online) M_N-H relationships for different temperatures at (a) $P = 0$ MPa and (b) 20 MPa in Fig. 3(a) Temperatures noted by color characters in (b) correspond to plots and dotted lines with the same color.

Mostly linear relationship in the H_{c2} vs T has been also confirmed. Superconducting coherence length has been estimated to be ~22 nm from the slope value. This is also in good agreement with those in Fig. 2 sample and Ref. 2. Moreover, hysteresis in the M_N-H curves could be observed on an increase and decrease in H. These behaviors are strong evidence for Meissner effect for type-II superconductivity as mentioned above and we turned out in Ref. 2. In contrast, small magnetization drop at $T \geq T_c = 8$ K is due to graphitic structure as mentioned above. All of these characteristics at $P = 0$ are qualitatively similar to tendency of Fig. 2 sample.

However, P dependence of T_c is much different from that in Fig. 2 sample. In contradiction to Fig. 2, as P slightly increases toward 20 MPa, T_c drastically increases up to 19 K in Fig. 3(a). This T_c value is as large as 2.4 times compared with $T_c = 8$ K at $P = 0$ MPa. Figure 4(b) shows M_N-H relationships for different temperatures at $P = 20$ MPa. They show behaviors with H_{c1} qualitatively similar to those in Fig. 4(a) and prove Meissner effect for type-II superconductivity. Such behaviors mostly disappear at $T = 20$ K and only

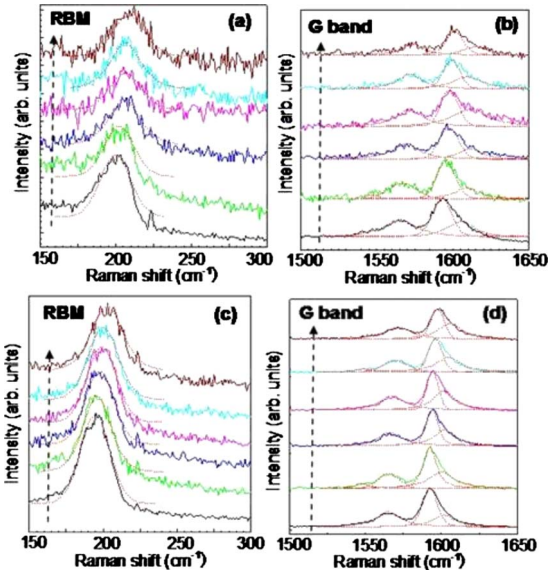

FIG. 5. (Color online) Pressure dependence of Raman spectra for samples shown in Fig. 1; [(a) and (b)] conventional film and [(c) and (d)] B-Buckypaper. Spectra were measured by an irradiating Ar laser of 488 nm wavelength at room temperature. P values are 0, 130, 380, 480, 570, and 760 MPa for (a) and (b), and 0, 210, 310, 380, 510, and 800 MPa for (c) and (d) from the bottom to the top curves. Red lines are results of data fitting by Gaussian-Lorentzian functions. For (a) and (b), only peaks were fit. For (c) and (d), three fitting functions were used.

a monotonic decrease in M_N with increasing H is observable at $T>20$ K. This supports that $T=19$ K can be a T_c for Meissner effect.

On the other hand, the M_N-H relationships in Fig. 4(b) are different from those in Fig. 4(a) in some detailed points as follows: (1) the feature at 10 K implies appearance of overlapping two M_N-H curves with the boundary P of $\sim$10 000 Oe, (2) the slope value of the M_N-H relationships at $H>H_{c1}$ decreases with increasing temperature, and, then, (3) H_{c2} values become very ambiguous and complicated as temperature increases. These are discussed in Sec. III based on electron-phonon coupling under pressure.

In Fig. 3(b), as P exceeds 20 MPa, M_N increases almost over the entire temperature region, and the T_c becomes unclear. These are qualitatively analogous to that observed in type-II SC above H_{c1} with increasing H. This indicates a possibility that SC area in the B-Buckypaper is compressed and becomes very thinner under applied pressure, resulting in partial penetration of the constant magnetic flux of $H=100$ Oe. Because volume fraction of the SC region can be estimated to be as small as less than 1%, this is possible.

Moreover, Fig. 3(b) indicates that graphitic diamagnetism appearing at $T>T_c$ does not become stronger with an increase in $P>20$ MPa in contradiction to that shown in Fig. 2. This behavior is consistent with the absence of ropes of the B-SWNTs in the B-Buckypaper as shown in Fig. 1(b) and supports the weak IVDW coupling among the B-SWNTs.

C. Pressure dependence of Raman spectrum

Here, we clarify the origin for the pressure-induced T_c in the Buckypaper shown in Fig. 3(a). Occurrence of the following two effects can be considered by applying pressure; (1) increase in phonon frequency and (2) decrease in charge transfer by the modulated B-C bonds.

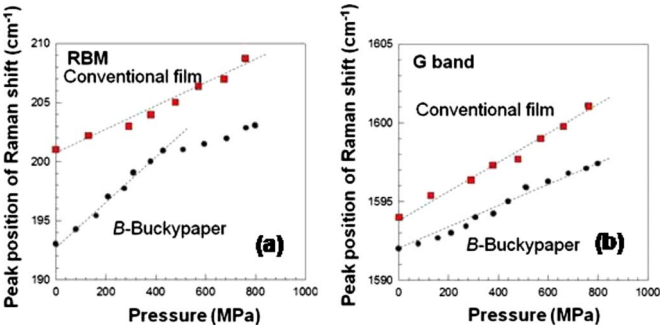

FIG. 6. (Color online) Peak positions vs pressure relationships in (a) RBM and (b) G-band mode. The peak positions were determined from the fitting peaks by red lines as shown in Figs. 5(a)–5(d). G-band peaks were selected from the highest peaks in (b) and (d). Ratios of range of Y/X axis are the same in both figures. Dotted lines are the results calculated by the method of least squares.

In order to reveal presence of (1), we explored the pressure dependence of the Raman spectra for the samples shown in Fig. 1. Figure 5 shows the results for (a) RBM and (b) G-band mode for the conventional film and for (c) and (d) for the B-Buckypaper. The RBM reflects the out-of-plane phonon along tube-diameter direction, and the G-band mode does the in-plane phonon along tube longitudinal direction.

Figure 6 shows peak positions vs pressure relationships in (a) RBM and (b) G-band mode determined from Fig. 5. From Figs. 5(b) and 6(a), it is evident that at $P=0$, all the peak positions observed for the B-Buckypaper are lower than those observed for the conventional film in both the RBM and the G-band mode. This trend is consistent with the observation in Fig. 1 [i.e., presence of as-grown ropes in Fig. 1(a) and its absence in Fig. 1(b)] and proves that strength of IVDW coupling in the Buckypaper is weaker than that in the as-grown ropes of SWNTs. This is because it is known that strong IVDW coupling makes the phonon frequency increase in ropes of SWNTs due to reduction in free vibration of lattices in individual SWNTs.[13,14]

With an increase in P, all the peak positions show a monotonic upshift for ratios of $\sim$1 cm^{-1}/100 MPa and $\sim$2 cm^{-1}/100 MPa in the RBM [Fig. 6(a)] and $\sim$0.7 cm^{-1}/100 MPa and $\sim$0.6 cm^{-1}/100 MPa in the G-band mode [Fig. 6(b)]. In particular, it should be noticed that only the RBM peak position for the B-Buckypaper in Fig. 6(a) shows the significantly high upshift ratio. It is as large as twice the upshift in RBM observed for the conventional film and three times larger than those for G-band modes. In contrast, this significant upshift saturates above $P=400$ MPa and the upshift ratio mostly becomes similar to those in others.

On the other hand, linewidth of $\sim$40 nm^{-1} for the RBM and $\sim$37 nm^{-1} for the G-band mode are common for both films and they are independent of P. Moreover, a peak around 1540 cm^{-1}, which was reported as a bundle effect for SWNT,[15] is not observable in both Figs. 5(b) and 5(d).

III. DISCUSSION

As explained in Sec. I, some theories have predicted that RBM is strongly coupled with σ-π band electrons in very thin SWNTs (e.g., diameters $\ll 1$ nm).[8] Here, Fig. 1(c) shows distribution of diameter of the B-SWNTs, which were used for the B-Buckypaper. It implies that B-SWNTs with diameter of 0.6 nm actually exist in ratio of $\sim$7%. Thus, the significant increase in RBM frequency in the B-Buckypaper shown in Fig. 6(a) can be a strong candidate for causes of the pressure-induced T_c.

When such very thin SWNTs were assembled together on the near place in the B-Buckypaper, the small area can yield Meissner loop current and, thus, exhibit pressure-induced T_c even under small pressure.

Indeed, volume fraction of superconducting region, which can be estimated from Fig. 3 ($\sim 10^{-5}$ emu/g), is as small as $\sim$1%. This is qualitatively consistent with $\sim$7% ratio of 0.6-nm-diameter SWNTs mentioned above because only a part of the B-SWNTs in the 5% ratio should become electrically active. Moreover, the volume fraction of 1% corresponds to an SC area of ~ 50 nm^2 in the present B-Buckypaper. This is also consistent with the superconducting coherence length of ~ 22 nm estimated for Fig. 4(a) as mentioned above.

Consequently, we conclude that the pressure-induced T_c observed in the B-Buckypaper [Fig. 3(a)] is attributed to the significant increase in the RBM phonon frequency caused by applying pressure shown in Fig. 6(a).

The significant increase in the RBM phonon frequency is also because the IVDW coupling in the B-Buckypaper is weaker than that in the as-grown ropes of SWNTs at $P=0$ as mentioned above and, thus, free lattice vibration for the RBM in individual SWNTs is not strongly restricted by IVDW coupling. As applied pressure increases, intertube spacing decreases and the IVDW coupling drastically increases only in the B-Buckypaper. Consequently, the RBM phonon frequency significantly upshifts only in the B-Buckypaper because the free lattice vibration is suppressed particularly for the RBM, which is the out-of-plane phonon mode along tube-diameter direction. When this suppression of the vibration for the RBM saturates at high P value, the upshift ratio in Fig. 6 should become the same as others. The saturation above $P=400$ MPa in the RBM as shown in Fig. 6(a) is in qualitatively good agreement with this interpretation.

As shown in Fig. 4(b), the slope value of M_N-H curves at $H > H_{c1}$ at $P=20$ MPa decreased and H_{c2} became ambiguous, as temperature increased. This was very different from those at $P=0$ MPa shown in Fig. 4(a) and also conventional type-II SC. This can be also interpreted from the increase in the RBM at $P=20$ MPa in the B-Buckypaper. As temperature increases, this increase in phonon frequency is induced under applied $P=20$ MPa. It tends to suppress destruction of SC region by magnetic flux. Hence, the slope value of M_N-H curves at $H > H_{c1}$ decreased at high temperatures.

In order to quantitatively reconfirm the conclusion, strong electron-phonon interaction must be experimentally identified for the 0.6-nm-diameter B-SWNTs in the Buckypaper because the applied pressure in Fig. 3(a) is as small as 20 MPa, which corresponds to only an the RBM frequency increase of 0.4 cm^{-1} in Fig. 6(a).[16] Moreover, it should be also reconfirmed that the RBM in Fig. 6(a) mainly originates from phonon of the 0.6-nm-diameter B-SWNTs. Furthermore, the p-independent linewidth with the common values for both films and the missing 1540 cm^{-1} peak mentioned in previous section are also not understandable.

On the other hand, although phonon modes of conventional films also slightly increase with applying pressure in Fig. 5, the T_c did not change in Fig. 2. This is due to reduction in the electron-phonon interactions in the rope structure. It is known that strong IVDW coupling in the rope structure weakens the electron-phonon coupling.[8]

As other origin for the pressure-induced T_c, a decrease in charge transfer caused by a reduction in the B-C bond under the applied pressure can also result in the improved alignment of E_F to a VHS. According to Refs. 2 and 9, even a small decrease in N_B (<1 at. %) and reduction in charge transfer make an alignment of E_F to a VHS improved, resulting in a drastic increase in EDOS and T_c. In fact, in B-doped diamond, T_c decreases under high pressures[6] because of the decrease in charge transfer in the B-C bonds. Thus, this phenomenon might occur also in the present B-Buckypaper, more or less.

IV. CONCLUSION

We showed formation of Buckypaper, which is a paperlike thin film consisting of pseudo-two-dimensional network of individual B-SWNTs, by sufficiently dissolving as-grown ropes of SWNTs and densely assembling them on silicon substrate. We found that T_c of 8 K under absent pressure could be induced as large as 2.4 times up to 19 K by applying a pressure as small as 20 MPa. A significant frequency increase in the RBM was also found with applying pressure in Raman spectrum measurements. Moreover, B-SWNTs with a diameter of 0.6 nm were confirmed in the Buckypaper. These implied the strong correlation of the pressure-induced T_c with electron-phonon (RBM) coupling of 0.6-nm-diameter B-SWNTs in the B-Buckypaper.

Further investigation of the causes for the pressure-induced T_c is necessary. However, the present results promise a possibility for obtaining T_c higher than 19 K in the B-Buckypaper by optimization of carrier concentration and film structures with applying pressure. In particular, an increase in volume fraction of SC regions consisting of thin B-SWNTs (diameter $\sim$0.5 nm) is expected to be effective. Moreover, it assures for producing flexible superconducting films valuable for transparent films and electronics.

ACKNOWLEDGMENTS

The authors thank H. Fukuyama, J. Akimitsu, M. Dresselhaus, S. Saito, R. Saito, T. Ando, H. Shinohara, S. Maruyama, S. Bandow, J. Gonzalez, A. Zakhidov, H. Bjorn, and T. Koretsine for the encouragement and for fruitful discussions.

*Author to whom correspondence should be addressed; j-haru@ee.aoyama.ac.jp

[1] J. A. Fagan, M. L. Becker, J. Chun, and E. K. Hobbie, Adv. Mater. **20**, 1609 (2008); Q. Cao, H.-s. Kim, N. Pimparkar, J. P. Kulkarni, C. Wang, M. Shim, K. Roy, M. A. Alam, and J. A. Rogers, Nature (London) **454**, 495 (2008).

[2] N. Murata, J. Haruyama, J. Reppert, A. M. Rao, T. Koretsune, S. Saito, M. Matsudaira, and Y. Yagi, Phys. Rev. Lett. **101**, 027002 (2008).

[3] See supplementary material at http://link.aps.org/supplemental/10.1103/PhysRevB.82.045402 for a summary of sample fabrication methods and identification for Meissner effect.

[4] T. E. Weller, M. Ellerby, S. S. Saxena, R. P. Smith, and N. T. Skipper, Nat. Phys. **1**, 39 (2005).

[5] N. Emery, C. Hérold, M. d'Astuto, V. Garcia, C. Bellin, J. F. Marêché, P. Lagrange, and G. Loupias, Phys. Rev. Lett. **95**, 087003 (2005).

[6] E. A. Ekimov, V. A. Sidorov, E. D. Bauer, N. N. Mel'nik, N. J. Curro, J. D. Thompson, and S. M. Stishov, Nature (London) **428**, 542 (2004).

[7] M. Kociak, A. Yu. Kasumov, S. Guéron, B. Reulet, I. I. Khodos, Yu. B. Gorbatov, V. T. Volkov, L. Vaccarini, and H. Bouchiat, Phys. Rev. Lett. **86**, 2416 (2001).

[8] R. Barnett, E. Demler, and E. Kaxiras, Phys. Rev. B **71**, 035429 (2005).

[9] T. Koretsune and S. Saito, Phys. Rev. B **77**, 165417 (2008).

[10] I. Takesue, J. Haruyama, N. Kobayashi, S. Chiashi, S. Maruyama, T. Sugai, and H. Shinohara, Phys. Rev. Lett. **96**, 057001 (2006).

[11] N. Murata, J. Haruyama, Y. Ueda, M. Matsudaira, H. Karino, Y. Yagi, E. Einarsson, S. Chiashi, S. Maruyama, T. Sugai, N. Kishi, and H. Shinohara, Phys. Rev. B **76**, 245424 (2007).

[12] M. Matsudaira, J. Haruyama, N. Murata, Y. Yagi, E. Einarsson, S. Maruyama, T. Sugai, and H. Shinohara, Physica E **40**, 2299 (2008).

[13] U. D. Venkateswaran, A. M. Rao, E. Richter, M. Menon, A. Rinzler, R. E. Smalley, and P. C. Eklund, Phys. Rev. B **59**, 10928 (1999).

[14] U. D. Venkateswaran, E. A. Brandsen, U. Schlecht, A. M. Rao, E. Richter, I. Loa, K. Syassen, and P. C. Eklund, Phys. Status Solidi B **223**, 225 (2001).

[15] R. Saito *et al.*, *Carbon Nanotubes*, edited by M. S. Dresselhaus, G. Dresselhaus, and Ph. Avouris (Springer-Verlag, Berlin, 2001).

[16] The measured pressure regions are different between Figs. 3 and 4 and Figs. 5 and 6 because in pressure-dependent Raman spectrum measurement for Figs. 5 and 6, the measurement system was unstable at $P<100$ MPa and we could not perform exact observation, in contradiction to the magnetization measurement for Fig. 3. However, mostly linear relationship starting from $P=0$ [dotted lines in Fig. 6(a)] implies that the upshift of RBM frequency can occur even at $P<100$ MPa.